Study regarding the compatibility between cellulose acetate (CA) and ZnO nanoparticles in polymeric membrane structures using functionalized m-phenylenediamine

M. Băjan, D. L. Cursaru *
Petroleum-Gas University of Ploieşti, Faculty of Petroleum Refining and Petrochemistry, Ploieşti

This study examines the effects of functionalized m-phenylenediamine (m-PDA-f) on the structure of cellulose acetate (CA) polymeric membranes enhanced with zinc oxide nanoparticles (ZnO). The membranes were prepared by dissolving cellulose acetate in an aprotic solvent, followed by a phase inversion process. The addition of m-PDA-f facilitates the formation of bridges between the cellulose acetate and ZnO nanoparticles. This is confirmed by FTIR analysis, which reveals a shift in the wavenumber of 3 to 5 cm^{-1}, highlighting an increase in the number of hydrogen bonds formed. Thermogravimetric analysis (TGA) confirms the enhanced stability of the membranes, with a significant increase in the thermal decomposition temperature: from 235 °C for pure cellulose acetate to 285 °C for the composite containing ZnO and the functionalized polymer. Differential scanning calorimetry (DSC) reveals lower enthalpy values for the membranes where m-PDA-f is present alongside ZnO. Furthermore, the best hydrophilicity was observed in the CA – m-PDA-f – ZnO membranes, exhibiting a contact angle of 34 degrees for water droplets, compared to 51 degrees for the membrane without the functionalized polymer. This demonstrates an increase in compatibility between the polymer and the nanomaterial through the formation of additional stable bonds.

(Received October 28, 2024; Accepted January 23, 2025)

Keywords: Membrane, Functionalized m-phenylenediamine, Zinc oxide nanoparticles, Stability, Compatibility

1. Introduction

Preserving and ensuring the quality of drinking water resources is a global concern in today's world. Research indicates that only 3% of the total water available is freshwater, which is found in ice caps, rivers, lakes, swamps, and underground sources. From an accessibility perspective, this percentage dwindles to a mere 0.3% [1]. Addressing the challenge of securing drinking water resources requires a comprehensive approach. The first step involves focusing on water quality by limiting the discharge of pollutants from industrial activities and advancing efficient treatment technologies. The second step involves prioritizing the careful use of freshwater resources.

When evaluating water quality, it is important to review the most notable classes of pollutants, including pharmaceutical pollutants, persistent organic pollutants (POPs), pesticides, organic chlorine and fluorine-based insecticides, polycyclic aromatic hydrocarbons (PAHs), and microbial pollutants [2].

The advancement of water purification technologies with enhanced efficiency is essential, given the variety of pollutants that enter the water and their harmful effects on the environment and organisms, along with the limited effectiveness of existing municipal or industrial treatment systems.

An accessible and efficient solution is membrane filtration, where the membrane acts as a selective barrier, allowing the passage of specific species from a solution. Membranes are categorized based on their pore size into microfiltration (pore sizes between 100 and 10000 nm),

* Corresponding author: dianapetre@upg-ploiesti.ro
https://doi.org/10.15251/DJNB.2025.201. 103

ultrafiltration (pore sizes between 100 and 1000 nm), reverse osmosis (pore sizes between 30 and 50 nm), and nanofiltration, which has pore sizes between those of ultrafiltration and reverse osmosis membranes [3,4].

Membranes can be made from various materials, including inorganic ones such as ceramic, metal, and quartz, as well as organic raw materials. The most commonly used polymers are cellulose acetate, polyamide, polysulfone, polyurethane, and cellulose triacetate. A membrane's efficiency is assessed based on factors such as permeate flow rate, the ability to maintain efficiency over multiple cycles until regeneration, mechanical strength, and selectivity for key contaminants [5].

Polymeric membranes offer several advantages over inorganic ones, including simple manufacturing technologies, low cost of raw materials, and the ability to control the diameter and distribution of pores. However, using the polymer alone may not guarantee superior filtration performance. One method to enhance efficiency is by incorporating nanomaterials but improving compatibility between the nanomaterial and the polymer requires functionalizing the nanometric structures to create more stable chemical interactions [6].

The properties of membranes that are enhanced by nanoparticles are attributed to their geometric features, such as a large surface area compared to volume, which enables them to retain more contaminants in between regeneration cycles. Additionally, nanomaterials exhibit photocatalytic properties that effectively target pollutants. Their role in slowing down biofouling and aiding in removing biological contaminants should also be duly acknowledged [7].

The interaction between nanomaterial and polymer is constrained by the existence of some functional groups, which facilitate the aggregation of it with the organic matrix and allow a uniform distribution [8].

M-phenylenediamine (mPDA) is a type of diamine with a good ability to treat wastewater by adsorbing pollutants, especially dyes. This reduces the need for nanocomposites with photocatalytic effects in water treatment devices such as photocatalysts and membranes. The hydrophilic nature of mPDA helps to increase the flow rate of water through the membrane structure. Additionally, the compatibility between mPDA polymer and cellulose acetate, facilitated by the amino and carboxyl groups, is a focus of the current study [9]

This study aims to assess the interactions between functionalized m-phenyldiamine (mPDA-f), cellulose acetate, and zinc oxide. The objective is to introduce a secondary polymer into the membrane structure, enhancing the compatibility of nanomaterials with cellulose acetate. This approach circumvents the need for nanoparticle functionalization, which often occurs under severe conditions (such as high pressure and temperature), is time-consuming, and must be tailored, to the specific type of nanomaterial.

The polymer is functionalized by grafting sulfate ions onto its structure, allowing it to interact with the oxygenated functional groups of cellulose acetate (carboxyl, carbonyl, and aldehyde). This interaction between the two polymers results in improved nanomaterial distribution and modifies the membrane's crystallinity, melting points, and hydrophilicity, compared to samples prepared solely from nanoparticles and cellulose acetate.

2. Experimental study

2.1. Materials

All reagents used in this study are purchased from Aldrich–Sigma and are reagent grade. Cellulose acetate (CA) as the base raw material for the membrane matrix, N,N-dimethylformamide (DMF) as solvent, zinc oxide (ZnO) nanoparticles (particle size < 100 nm), m-phenylenediamine (m-PDA) monomer subjected to polymerization and functionalization, 98% concentrated sulfuric acid (H_2SO_4), 37% concentrated hydrochloric acid, for the initialization of mPDA polymerization, and ammonium sulfate $(NH_4)_2SO_4$ were also employed.

2.2. Synthesis of samples

2.2.1. Obtaining the mPDA-f polymer

The polymerization of m-PDA began by dissolving 1.08g of monomer in a 20 ml solution containing 1.6 ml of concentrated sulfuric acid. The mixture underwent mechanical agitation for 5

hours at 200 rotations per minute (rpm) at a constant temperature of 40 °C. Functionalization involved addition of 15 ml ammonium sulfate solution (10%) to the polymer solution and stirring for another 3 hours under the same conditions. The solid phase was filtered and washed first with 15 ml of 2 M HCl, and then with 100 ml of distilled water.

The obtained polymer was dried in a vacuum at a temperature of 60 °C for 6 hours. This method was based on data presented by Siddhartha et al., who investigated the polymerization of o-phenylenediamine in various inorganic acid media (hydrochloric acid, phosphoric acid, and sulfuric acid). Our study aims to obtain the polymer m-phenylenediamine, based on literature data investigating the polymerization of o-phenylenediamine in the presence of sulfuric acid. Structurally, the obtained polymer is soluble in DMF due to the open ring, a behavior also reported in the literature [10].

2.2.2. Obtaining membranes

Cellulose acetate membranes were obtained by phase inversion in a nonsolvent (water). To incorporate ZnO nanoparticles, the cellulose acetate granules were dispersed in DMF solvent by mechanical stirring for 30 minutes at 400 rpm, after which the CA granules were added. After their complete dissolution, the formed gel was left to settle at room temperature (20 °C) for 24 hours, to remove air bubbles. The membranes containing the functionalized polymer were prepared by dispersing mPDA-f in solvent along with nanoparticles, under the same stirring conditions, followed by the addition of cellulose acetate.

The formed gels were stacked on the surface of a glass plate and evenly dispersed through centrifugal force. Solidification was done by immersing the membrane in distilled water. The composition of the manufactured membranes Is presented in table 1.

Table 1. Mass of each element in the composition of membranes.

Membrane type	CA (g)	ZnO (g)	m-FDA-f (g)	DMF (ml)
CA	1	-	-	5
CA, ZnO	1	0.1	-	5
CA, m-PDA-f	1	-	0.2	5
CA, m-PDA-f, ZnO	1	0.1	0.2	5

2.3. Sample characterization

For the qualitative analysis of the materials, *FTIR spectroscopy* was used to identify the functional groups in the structure. The equipment used was Shimadzu IRAffinity-1S spectrophotometer (Kyoto, Japan), equipped with the GladiATR-10 accessory. The determination was made in the range of wavelengths 800 - 3000 cm-1, at a spectral resolution of 4 cm-1.

Thermogravimetric analyses (TGA) of the materials were recorded on a TGA, using Labsys Evo apparatus from Setaram (Caluire, France), in the 20–900 °C temperature range, in a nitrogen atmosphere, with a heating rate of 5 °C/min.

Differential scanning calorimetry (DSC) was made to study the temperature-induced transition, such as melting, respectively the occurrence of the glassy state. The equipment used was Thermal Analysis System DSC 3+ from Mettler Toledo (Greifensee, Switzerland). The heating was done from room temperature to 400 °C with a heating rate of 10 °C/min in a nitrogen atmosphere.

The goniometric analysis (GA) highlighted the contact angle made by the water droplet with the surface of the membranes. A drop of distilled water, volume (10µl) was placed on the surface of the sample, and its image was taken using the Intel Play QX3 USB Digital Microscope camera (China). The value of the contact angle that the water drop makes, gives information about the hydrophilicity of the samples.

3. Results and discussions

3.1. FTIR analysis

FTIR analysis was performed both for the mPDA monomer and for the functionalized polymer (mPDA-f), to highlight the presence of sulfate groups in its structure. According to Figure 1, the stretching vibration at 1050 cm^{-1} shows degrees of sulfonation greater than 1.5 [11]. After functionalization, the presence of bending vibrations associated with amino groups for m-FDA disappears, as a result of their interaction with sulfate ions. The intensity of the bands observed at 1585 cm^{-1} specific to the fingerprint decreases as a result of the aggregation of the aromatic cycles, a behavior that confirms the formation of the polymer. The stretching band observed at 3390 cm^{-1}, in the case of the functionalized polymer, marks the presence of oxygen atoms attributed to sulfate functional groups. The spectrum obtained for the PDA polymer is in agreement with the one presented by Svoboda et al. [12] which highlights the presence of aromatic cycles through the bands in the range 1380 cm^{-1} ÷ 1600 cm^{-1}, respectively of the stretching vibrations between C-C and C-N.

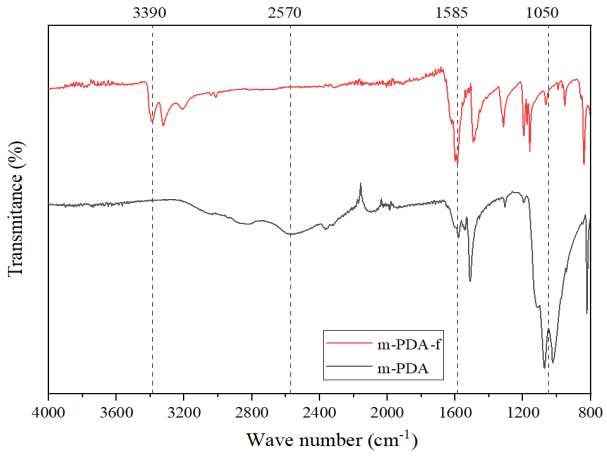

Fig. 1. FTIR spectrum of m-phenylenediamine before and after polymerization and functionalization.

The FTIR graph from Figure 2 shows stretching vibrations at 3480 cm^{-1} assigned to the hydrogen bonds made between the hydroxyl groups (-OH). The stretching vibration at 1050 cm^{-1} are attributed to the C-O-C structures. The presence of ZnO increases the number of hydrogen bonds between the hydroxyl groups of cellulose acetate and zinc oxide nanoparticles, marked by stretching vibrations from 1230 cm^{-1}.

The values obtained for the cellulose acetate membranes, as well as cellulose acetate with zinc oxide nanoparticles, are consistent with those reported in the literature [13, 14]. When ZnO is added to the membrane, the wave number shifts by 3 to 5 units, as indicated in the current study [15]. The displacement of the peaks is more pronounced in the presence of mPDA-f due to the formation of complexes with greater stability between cellulose acetate and nanoparticles. At the same time, the presence of mPDA-f in the CA membrane and the CA-ZnO structure leads to a higher transmittance value at the wave number 1050 cm-1, attributed to the interactions between the sulfate and the oxygenated functional groups of cellulose acetate.

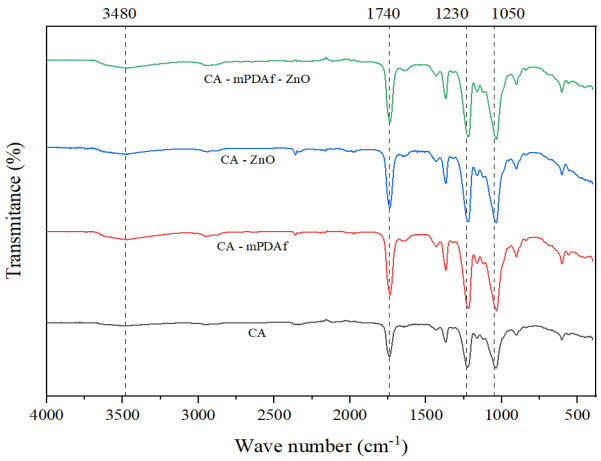

Fig. 2. FTIR spectrum of the membranes.

The spectrum for the CA-mPDA-f-ZnO membrane shows an increase in transmittance at 1740 cm^{-1}. This increase is caused by the formation of additional bonds between the positively charged nitrogen ions in the mPDA-f and the electronegative oxygen ions in the cellulose acetate (specifically the free C=O), as well as the oxygen from the ZnO nanoparticles. This demonstrates a strengthening of the interactions between cellulose acetate and nanoparticles through the formation of additional hydrogen bonds.

3.2. TG analysis

The mass losses of CA, CA – ZnO, CA – mPDA-f, CA – mPDA-f – ZnO membranes were studied comparatively. The mass loss noted up to the temperature of 100 °C is approximately 3% wt. for all samples and corresponds to the evaporation of water adsorbed in the structure.

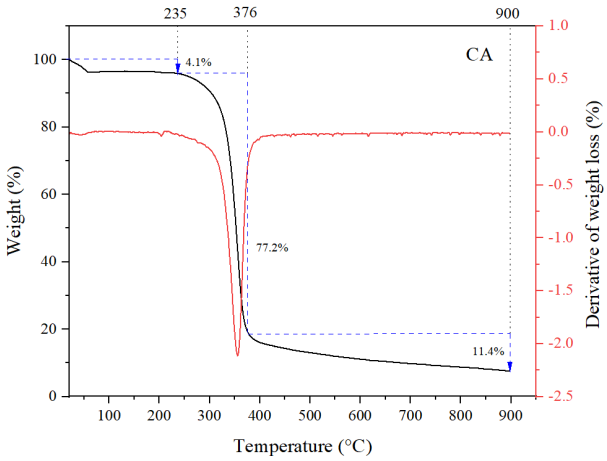

Fig. 3. TGA/DTA profile for cellulose acetate (CA) membrane.

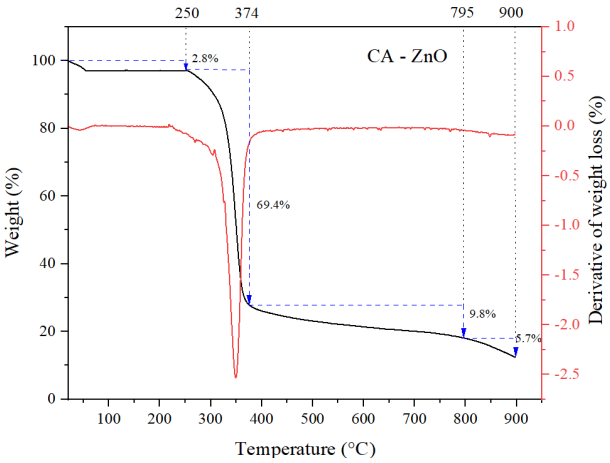

Fig. 4. TGA/DTA profile for cellulose acetate membrane with zinc oxide nanoparticles.

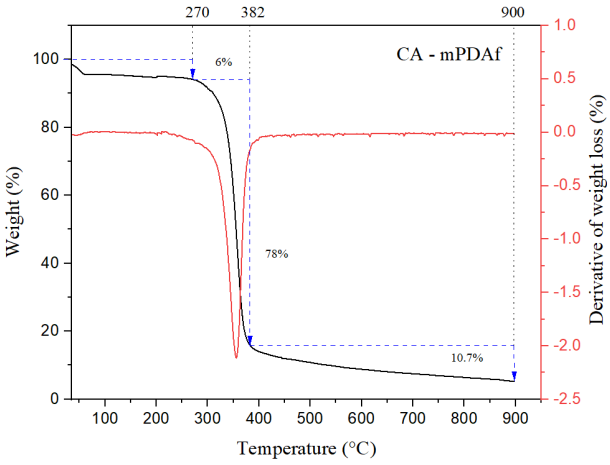

Fig. 5. TGA/DTA profile for cellulose acetate membrane with functionalized m-phenylenediamine.

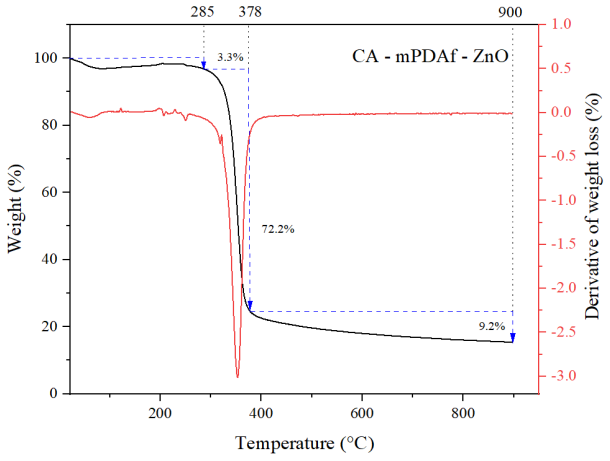

Fig. 6. TGA/DTA profile for cellulose acetate membrane with functionalized m-phenylenediamine and zinc oxide nanoparticles.

According to the data presented in Figure 3, the sample with CA leads to a sudden loss of mass starting at 240 °C, while the TGA variation shown in Figure 5 for membrane CA – mPDA-f knows the initiation of decomposition at 270 °C. The best values in this first range are for CA – mPDA-f – ZnO (figure 6), as a result of additional stable bonds, mediated by the functionalized polymer between cellulose acetate and ZnO.

The second thermal decomposition interval ends for all samples at approximately 375 °C. However, the mass loss obtained in the CA – mPDA-f – ZnO analysis is only 72.2% wt, while the CA – mPDA-f membrane has a mass loss of 78% wt. This difference in behavior is attributed to the presence of ZnO and the ability of the polymer to mediate the interaction between CA and zinc oxide. The mass loss is associated with the decomposition of functional groups of carbonyl, carboxyl, or acetate type contained in CA [13,16].

The delayed onset of decomposition in the presence of m-phenylenediamine is due to the stable hydrogen bonds formed between the functional groups of cellulose acetate and the functionalized amine polymer. The DTA curve indicates mass loss at 350 °C, attributed to the decomposition of organic matter.

The third thermal decomposition range occurs between 375°C and 900°C. In figure 4, the CA-ZnO membrane experiences a sudden mass loss between 795°C and 900°C, resulting in approximately 7% weight loss. This is attributed to the weakening of interactions between the nanomaterial and the cellulose acetate. Ultimately, only the metal that has transitioned into its crystalline form remains undecomposed. The CA-ZnO-mPDA-f structure demonstrates the lowest degree of decomposition, approximately 9.2% weight loss, indicating better stability of nanomaterials in the polymer network.

3.3. DSC analysis

DSC analysis highlights the transitions that occur in the membrane structure with temperature. Figure 7 shows the phase transformations experienced by the membranes: CA, CA – ZnO, CA – mPDA-f, CA – mPDA-f – ZnO.

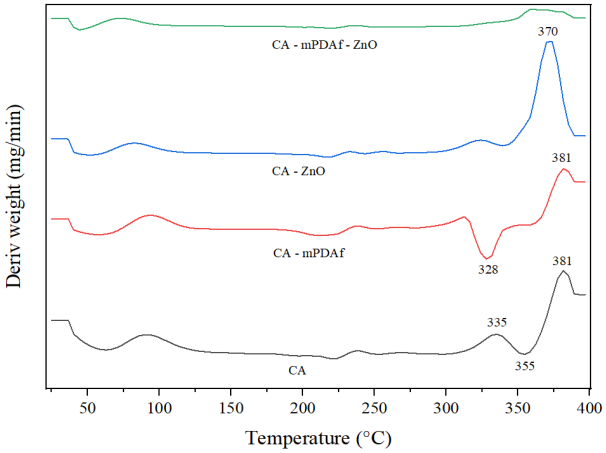

Fig. 7. DSC profile of the membranes.

The results for the CA-ZnO membrane indicate an endothermic transformation occurring between 25°C and 75°C, attributed to the loss of water from the sample. This transformation overlaps with the glass transition temperature [17,18]. The melting temperature is not clearly defined, supporting the formation of strong chemical bonds between the acetate functional groups, mediated by zinc oxide. Significant changes are observed at 390°C, confirming thermal decomposition.

The CA-mPDA-f-ZnO sample undergoes chemically bound water loss and transformation from the amorphous state to the crystalline state in the temperature range of 25°C to 75°C. This transformation is characterized by a slightly higher endothermic value, indicating a high degree of molecular disorder attributed to the intercalation of the functionalized polymer between the acetate groups. Additionally, there is a reduction in the degree of thermal decomposition at this temperature range. The presence of mPDA-f limits the thermal oxidation caused by oxygen in ZnO, leading to reduced endothermicity compared to other samples. Ultimately, the polymer's presence prevents the fragmentation caused by thermal oxidation.

3.4 Goniometric analysis

The contact angle was measured for all four samples. According to Figure 8, the CA-ZnO structure has the highest contact angle value at 51 degrees. In this case, the nanomaterial on the surface of the polymer reduces permeability by decreasing the number of available hydroxyl and carboxyl groups, thus lowering their weight [19,20].

Functionalized polymer mixed with CA reduces membrane hydrophilicity. The behavior is explained by the decrease in the number of available oxygen groups and the formation of networks with greater complexity than cellulose acetate. The membrane with CA leads to the formation of a water droplet angle of 47 degrees. By adding mPDA-f, is obtained the increase up to 50 degrees.

The addition of mPDA-f to the mixture of CA and ZnO resulted in significant changes in the membrane's angle. This structure showed greater hydrophilicity compared to the other membranes due to the increased distance between the polymers and the interactions of the oxygen in the nanoparticles with the amino groups in the functionalized polymer.

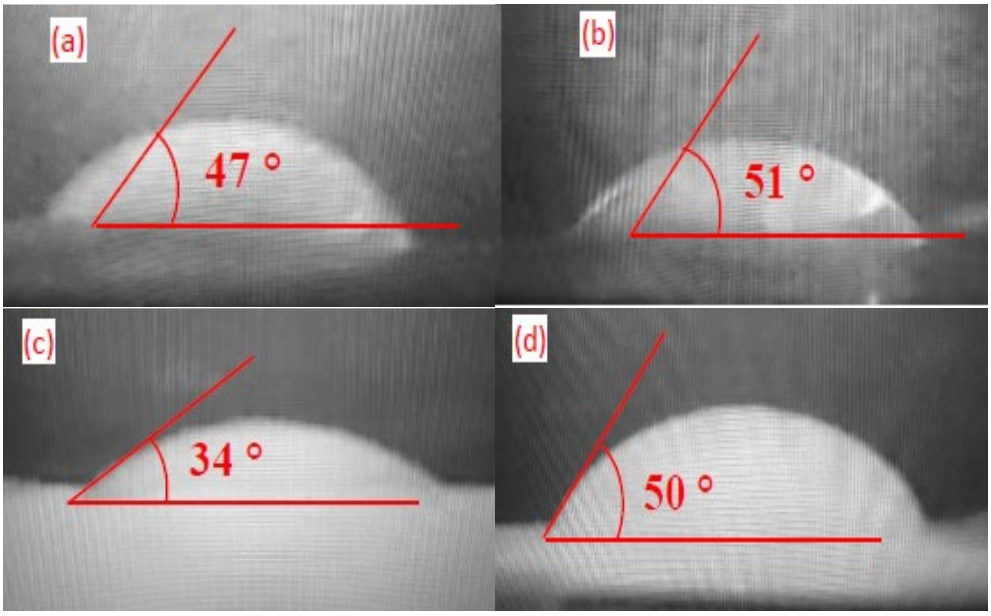

Fig. 8. The value of the contact angle of the water droplet with the surface of the membranes: (a) CA; (b) CA – ZnO; (c) CA – mPDA-f – ZnO; (d) CA – mPDA-f.

4. Conclusions

In this study, we analyzed the changes in the structure of cellulose acetate and zinc oxide membranes when a secondary polymer is used to increase compatibility between the organic and inorganic phases. The FTIR results of the analyzed samples show a shift in the wave number by 3÷6 units in the case of membranes containing mPDA-f, indicating an intensification of the number of hydrogen bonds.

The thermogravimetric analysis reveals that the second level of thermal decomposition begins at 285°C, the highest value among the samples analyzed. Additionally, the percentage indicating the mass loss in the third thermal decomposition level reaches the lowest values. These observations can be attributed to the increased interactions between the nanomaterial and the functionalized polymer, as well as between the polymer and the functional groups of cellulose acetate.

DSC analysis confirms an improved molecular distribution, with a reduction in thermal decomposition recorded at 370°C for the cellulose acetate membrane with zinc oxide nanoparticles. Goniometric tests show that the CA-mPDA-f-ZnO has the lowest contact angle (34 degrees), indicating increased hydrophilicity.

This study highlights the ability of the functionalized m-phenylenediamine polymer to immobilize ZnO nanoparticles and increase strong electrostatic interactions with cellulose acetate when the inorganic phase is introduced into the membrane structure. These structural changes pave the way for future studies on filtration efficiency, permeate flow rate, concentration polarization effect, and contaminant nature.

References

[1] Shi X., Mao D., Song K., Xiang H., Li S., Wang Z., Xinying S., Mao D., Water Research 260, 2024;121946; https://doi.org/10.1016/j.watres.2024.121946
[2] Ighalo J. O., Yap P. S., Iwuozor K.O., Aniagor O. C., Liu T., Dulta K., Felicitas U. Iwuchukwu F. U., Rangabhashiyam S., Environmental Research, 2022;212:113123; https://doi.org/10.1016/j.envres.2022.113123
[3] Baig U., Faizan M., Waheed A., Advances in Colloid and Interface Science; 2022;303:102635. https://doi.org/10.1016/j.cis.2022.102635
[4] Liu J., Zhang R., Wang L., Liu Y., Tian X., Dai X., Pan J., Dai J., Separation and Purification Technology, 2023;319:124051; https://doi.org/10.1016/j.seppur.2023.124051
[5] Burugaa K., Songb H., Shangc J., Boland N., Kalathia J. T., Kimd KI., Journal of Hazardous Materials, 2019;379:120584; https://doi.org/10.1016/j.jhazmat.2019.04.067
[6] He H., Shen X., Nie Z., Progress in Polymer Science, 2023;143:101710; https://doi.org/10.1016/j.progpolymsci.2023.101710
[7] Mo J., Li X., Yang Z., Separation and Purification Technology, 2024;345;127366. https://doi.org/10.1016/j.seppur.2024.127366
[8] Darabi R.R., Peyravi M., Jahanshahi M., Chemical Engineering Research and Design, 2019;145;85-98; https://doi.org/10.1016/j.cherd.2019.02.019
[9] Mousa H., El-Hay S.S.A., Sheikh R.E., Gouda A.A., El-Ghaffar S.A., El-Aal M.A., International Journal of Biological Macromolecules, 2024;258;128890; https://doi.org/10.1016/j.ijbiomac.2023.128890
[10] Amer I., Mokrani T., Jewell L., Young D.A., Vosloo H.C.M., Polymer, 2015;66;230-239; https://doi.org/10.1016/j.heliyon.2022.e12401
[11] Hu C.H., Weber M., Huang Y.H., Lai J.Y., Chung T.S., Journal of Membrane Science, 2024;705;122890; https://doi.org/10.1016/j.memsci.2024.122890;
[12] Svoboda J., Kral M., Dendisova M., Matˇejka P., Georgievski O.P., Colloids and Surfaces B: Biointerfaces, Colloids and Surfaces B: Biointerfaces, 2021;205;111897; https://doi.org/10.1016/j.colsurfb.2021.111897
[13] Algahtani F.D., Laput V., Atique S., Hamdi A., Snoussi M., Zrieq R., El-Morsy M.A., Materials Chemistry and Physics, 2024;323;129605; https://doi.org/10.1016/j.matchemphys.2024.129605
[14] Mousa H., El-Hay S.S.A., El Sheikh R., Gouda A.A., El-Ghaffar S.A., El-Aal M.A., International Journal of Biological Macromolecules, 2024;258;128890; https://doi.org/10.1016/j.ijbiomac.2023.128890
[15] Alhalili Z., Romdhani C., Chemingui H., Smiri M., Journal of Saudi Chemical Society, 2021, 25, 101282; https://doi.org/10.1016/j.jscs.2021.101282

[16] Alahmadi N., Hussein M.A., Journal of materials research and technology 2022;21;4409-4418; https://doi.org/10.1016/j.jmrt.2022.11.055
[17] Ali M., Zafar M., Jamil T., Butt M. T. Z., Desalination, 270;2011;98-104; https://doi.org/10.1016/j.desal.2010.11.027
[18] Taib M. N. A. M., Hamidon T. S., Garba N. Z., Trache D., Uyama H., Hussin M. H., Polymer, 244;2022;124677; https://doi.org/10.1016/j.polymer.2022.124677
[19] Maurya K.R.A., Chikkattib S.B., Sajjanb M. A., Banapurmathc R. N., Khand T.M.Y., Saleeld C. A., Next Energy; https://doi.org/10.1016/j.nxener.2024.100178
[20] Elaissaoui I., Sayeb S., Ounif I., Ferhi M., Karima H., Ennigrou D. J., Heliyon, 10;2024;e32552; https://doi.org/10.1016/j.heliyon.2024.e32552